

Supplementary Information

PDGFR α plays a crucial role in connective tissue remodeling

Shinjiro Horikawa^{1,2}, Yoko Ishii¹, Takeru Hamashima¹, Seiji Yamamoto^{1,*}, Hisashi Mori³, Toshihiko Fujimori⁴, Jie Shen¹, Ran Inoue³, Hirofumi Nishizono⁵, Hiroshi Itoh⁶, Masataka Majima⁷, David Abraham⁸, Toshio Miyawaki^{2,9}, and Masakiyo Sasahara¹

¹Department of Pathology, Graduate School of Medicine and Pharmaceutical Sciences, University of Toyama, Toyama 930-0194, Japan

²Department of Pediatrics, Graduate School of Medicine and Pharmaceutical Sciences, University of Toyama, Toyama 930-0194, Japan

³Department of Molecular Neuroscience, Graduate School of Medicine and Pharmaceutical Sciences, University of Toyama, Toyama 930-0194, Japan

⁴Division of Embryology, National Institute for Basic Biology, Okazaki 444-8787, Japan

⁵Division of Animal Experimental Laboratory, Life Science Research Center, University of Toyama, Toyama 930-0194, Japan

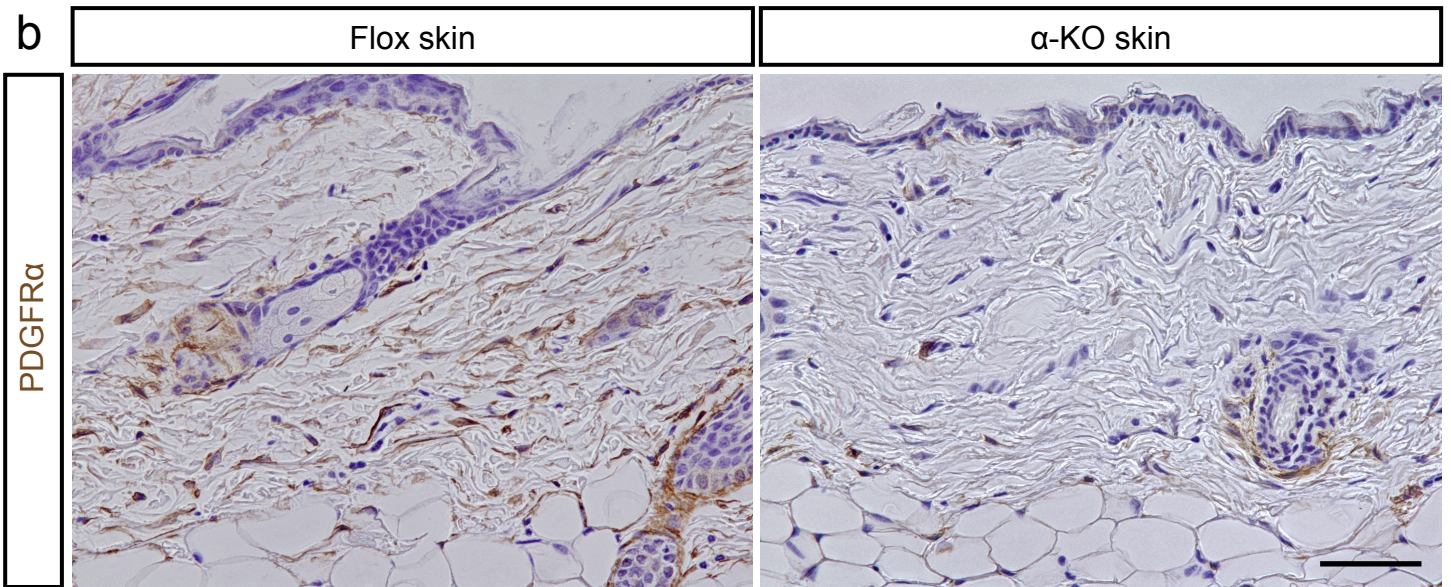
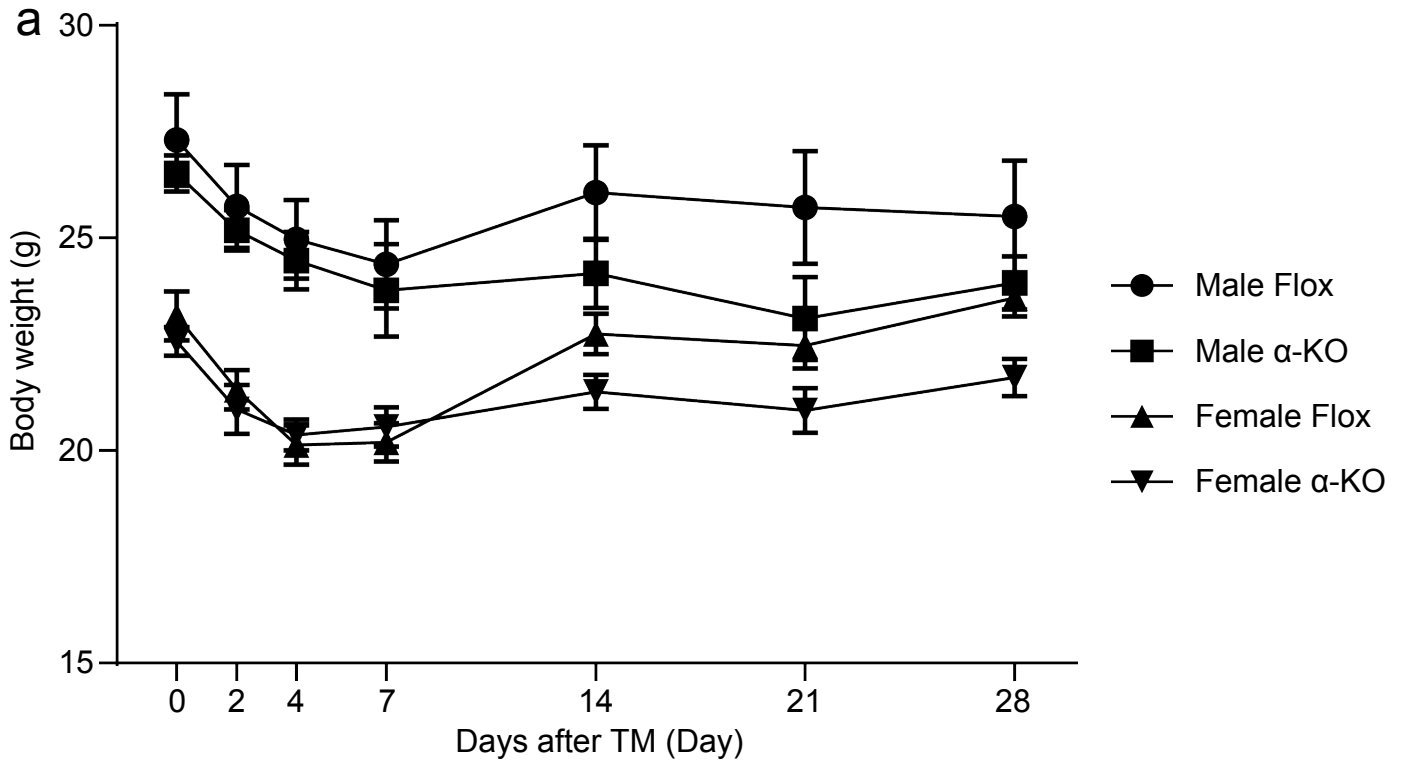
⁶Department of Molecular Pathology, Graduate School of Medicine, Yamaguchi University, Ube 755-8505, Japan

⁷Department of Pharmacology, School of Medicine, Kitasato University, Kanagawa 252-0374, Japan

⁸Division of Medicine, University College London, Royal Free Campus, London, NW3 2PF, UK

⁹Deceased, we dedicate this article to the memory of a brilliant and beloved colleague

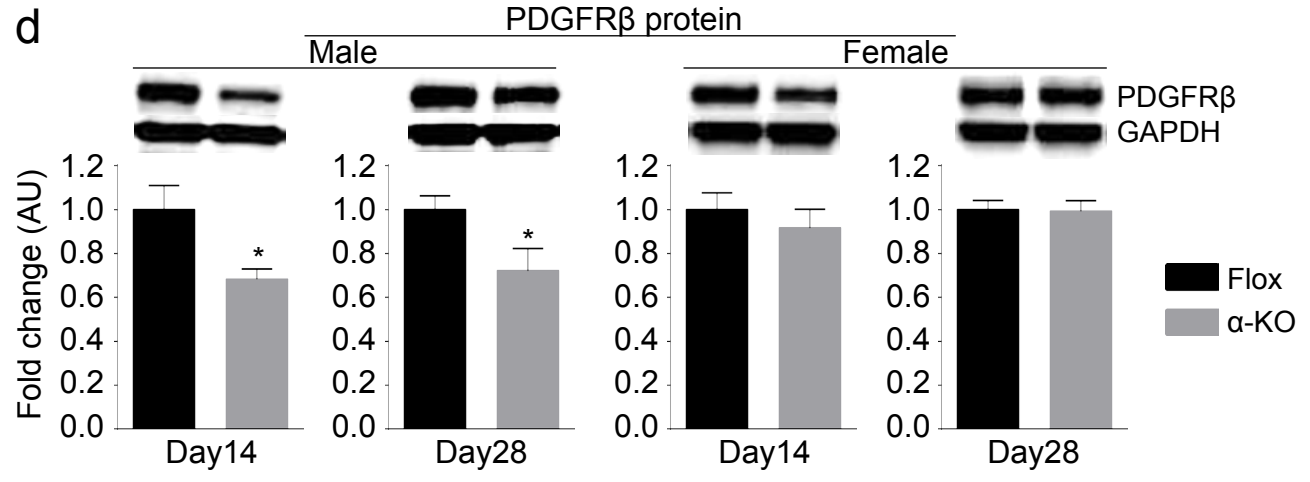
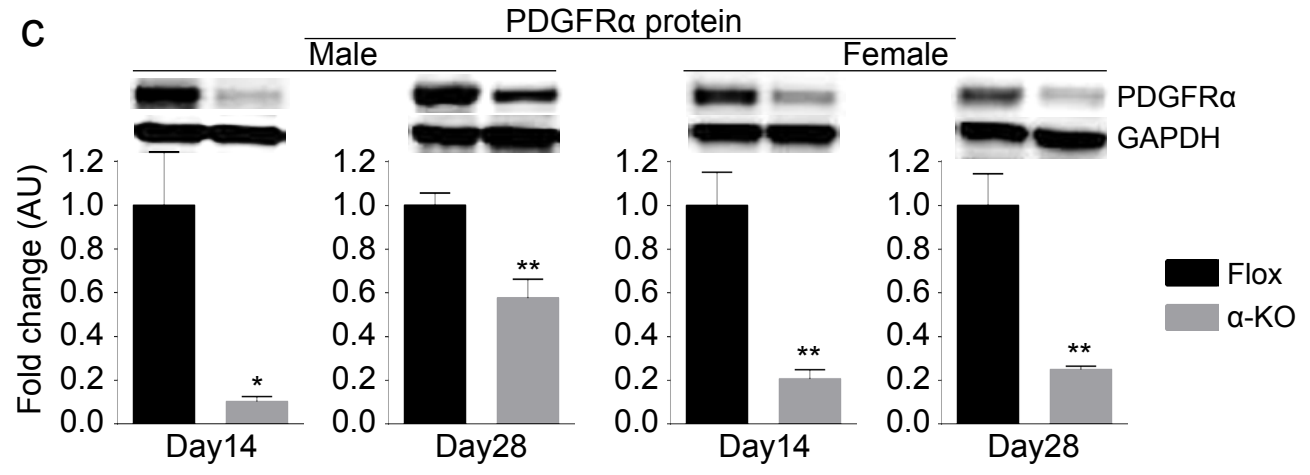
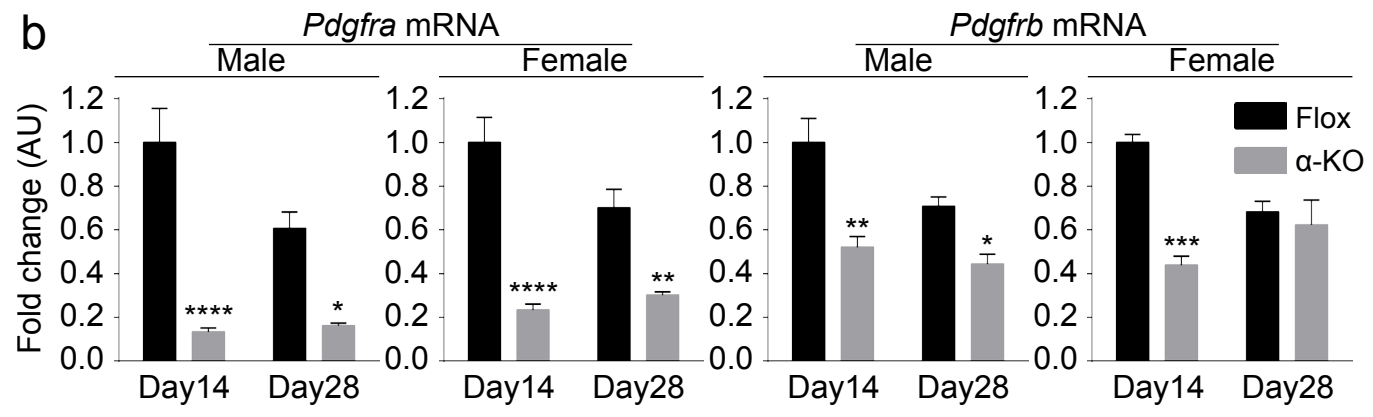
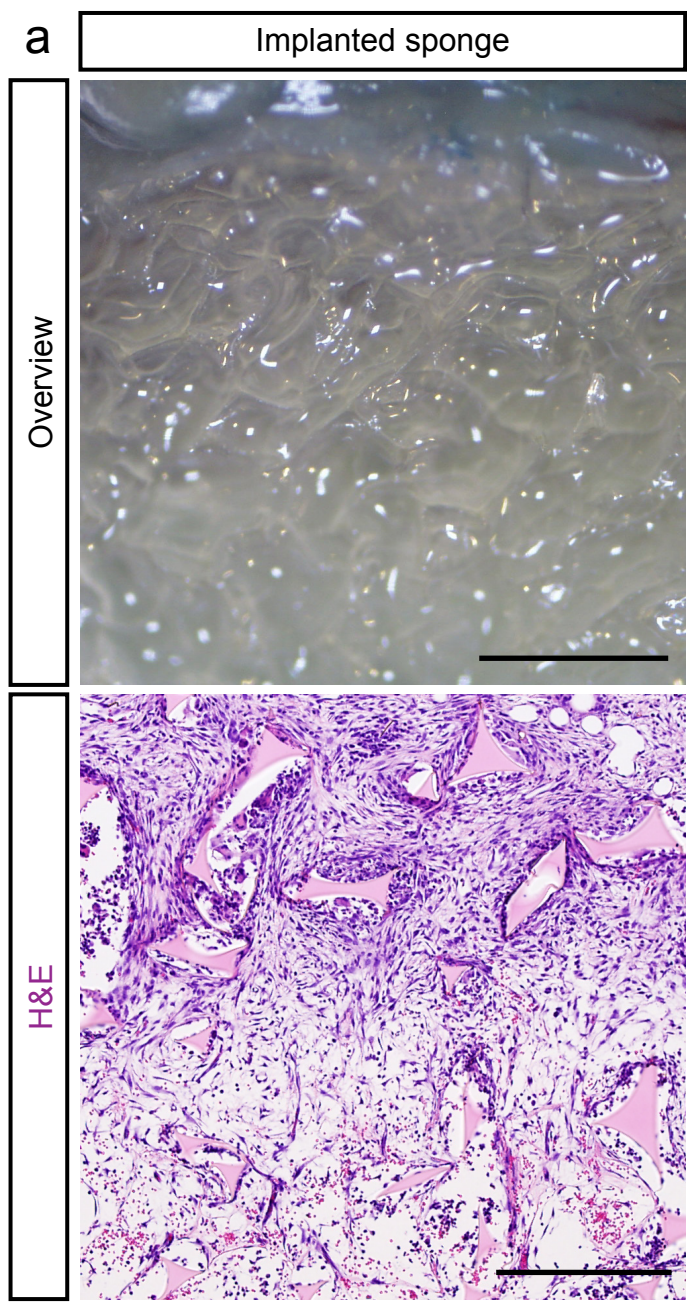
*Correspondence to: Seiji Yamamoto, Ph.D., Department of Pathology, Graduate School of Medicine and Pharmaceutical Sciences, University of Toyama, Toyama 930-0152, Japan
Tel: +81-076-434-2281, Fax: +81-076-434-5016, E-mail: seiyama@med.u-toyama.ac.jp



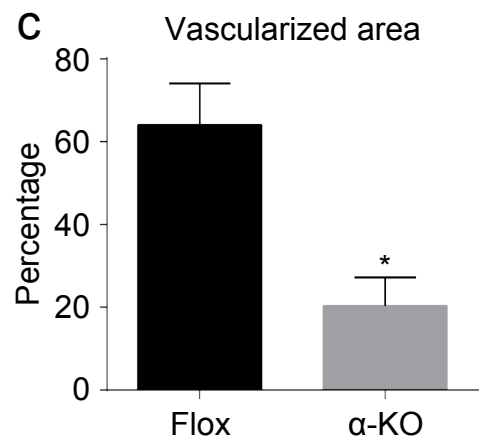
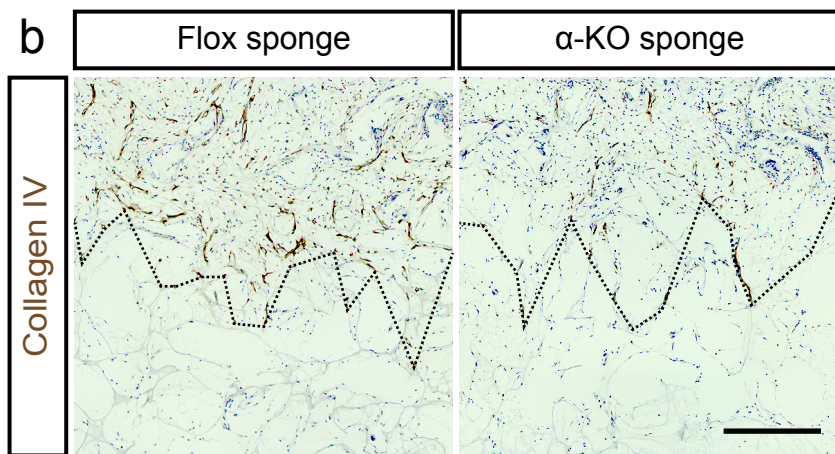
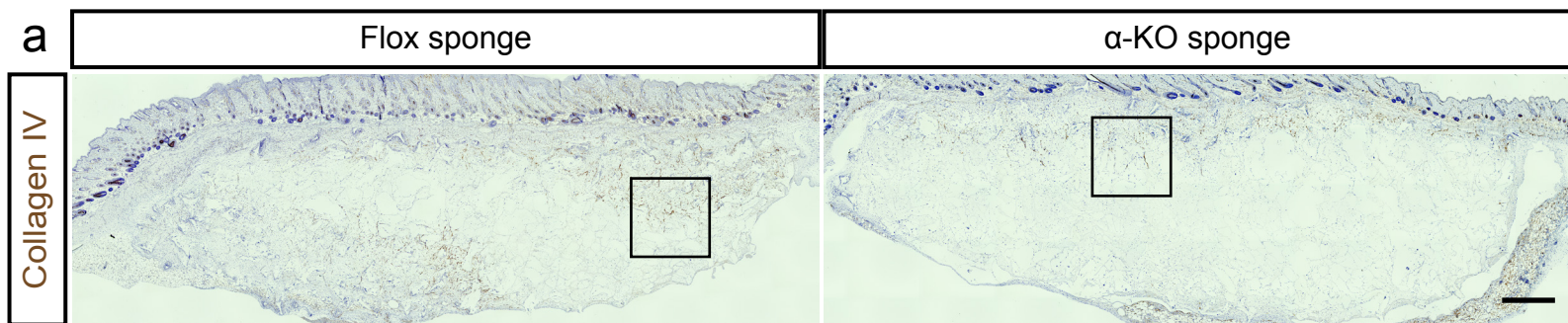
Supplementary Figure 1 | Sponge implantation model in PDGFR α -inactivated (α -KO) mice.

(a) The change in the body weights of male Flox mice (n = 12), male α -KO mice (n = 11), female Flox mice (n = 11), and female α -KO mice (n = 11) throughout experiments. (b)

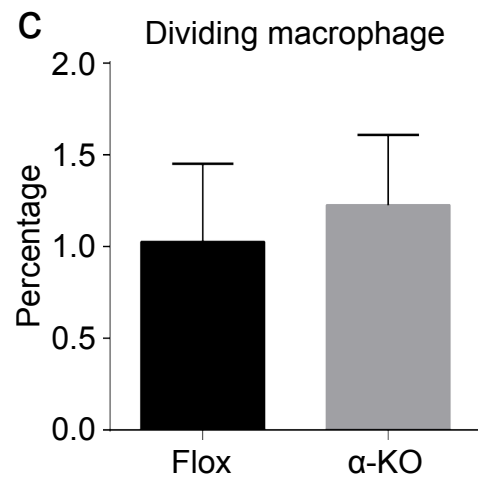
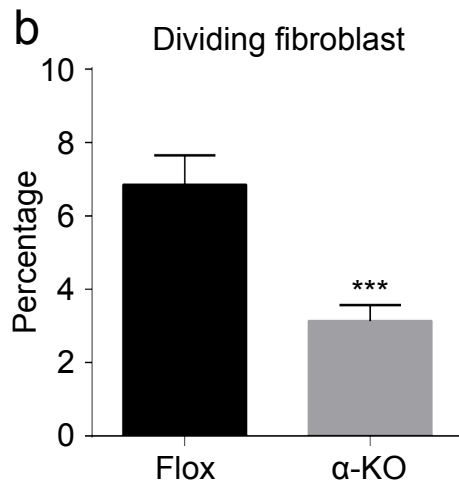
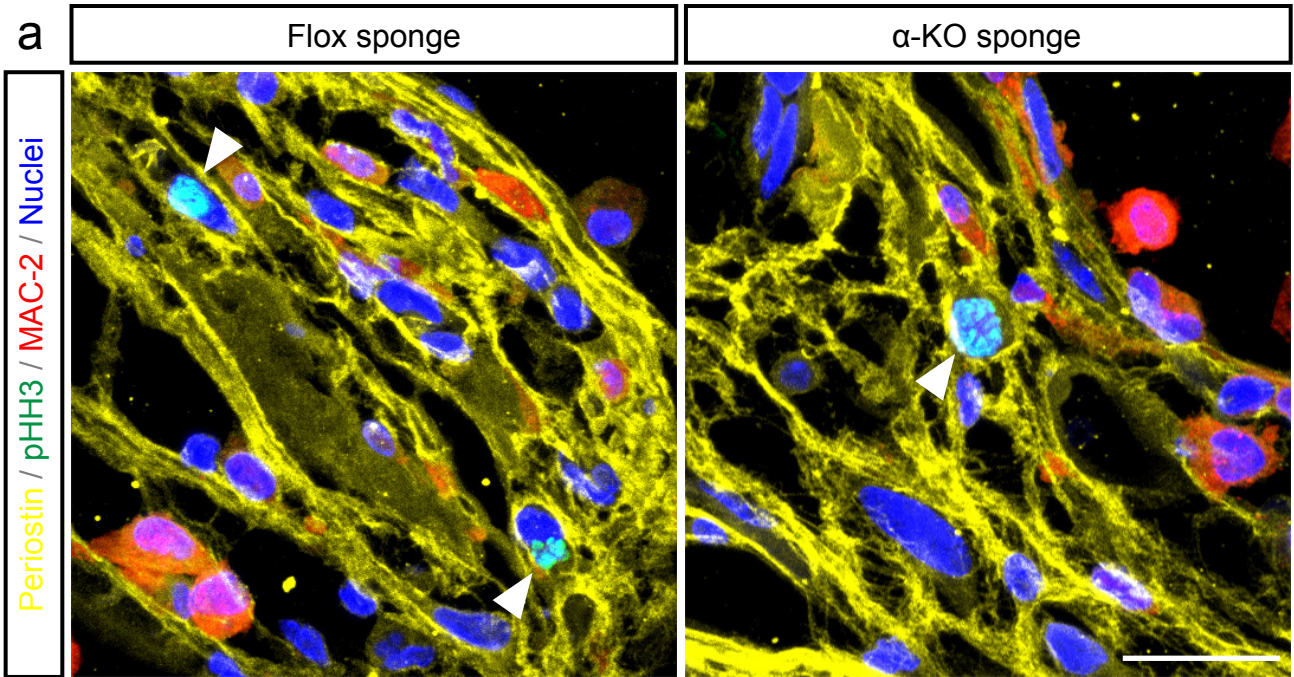
Immunohistochemistry of PDGFR α (brown) in Flox mice skin as a positive control (left), and α -KO mice (right) at 14 days after tamoxifen treatment for 5 consecutive days. Sections were counterstained with hematoxylin (pale blue). Scale bar indicates 50 μ m.



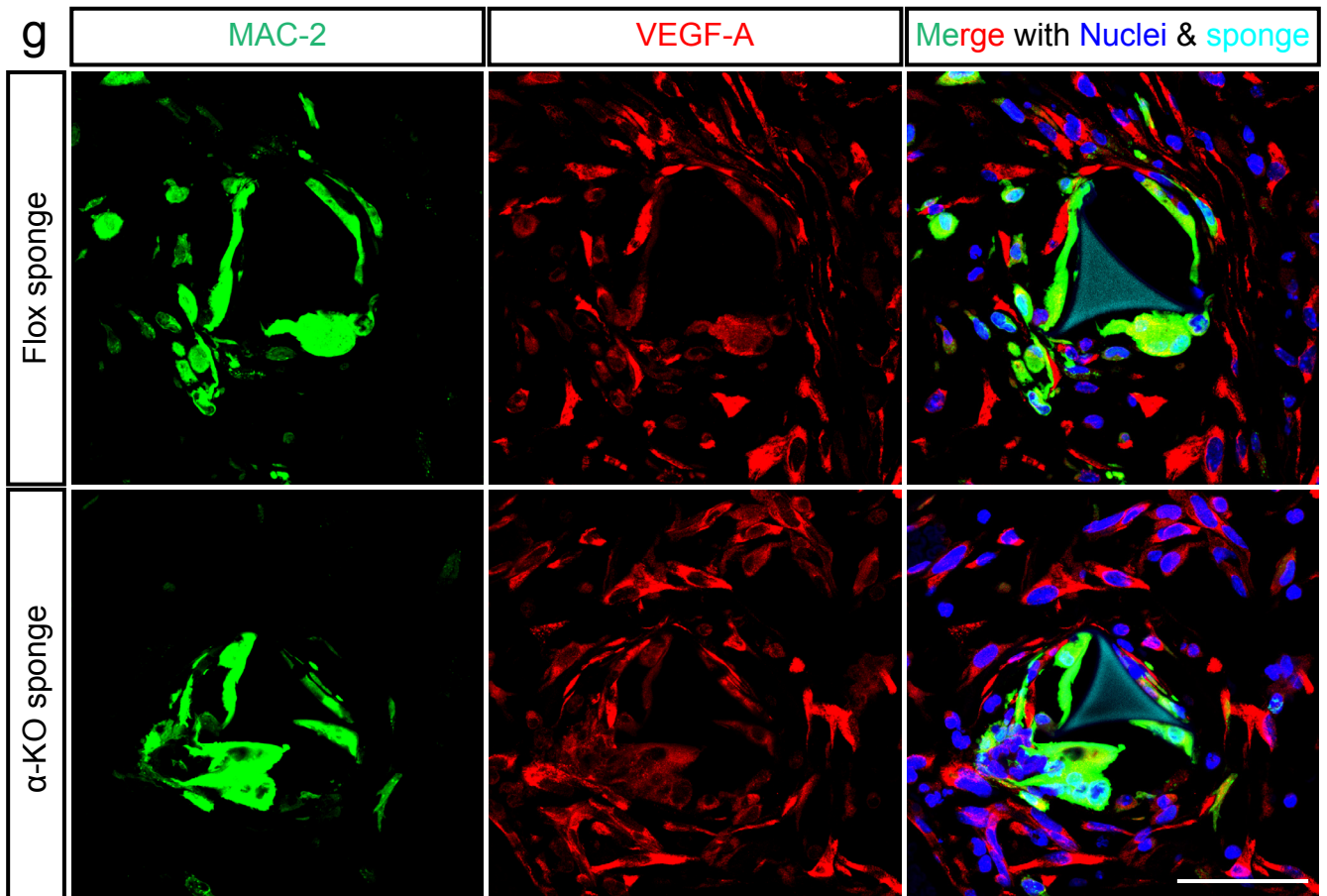
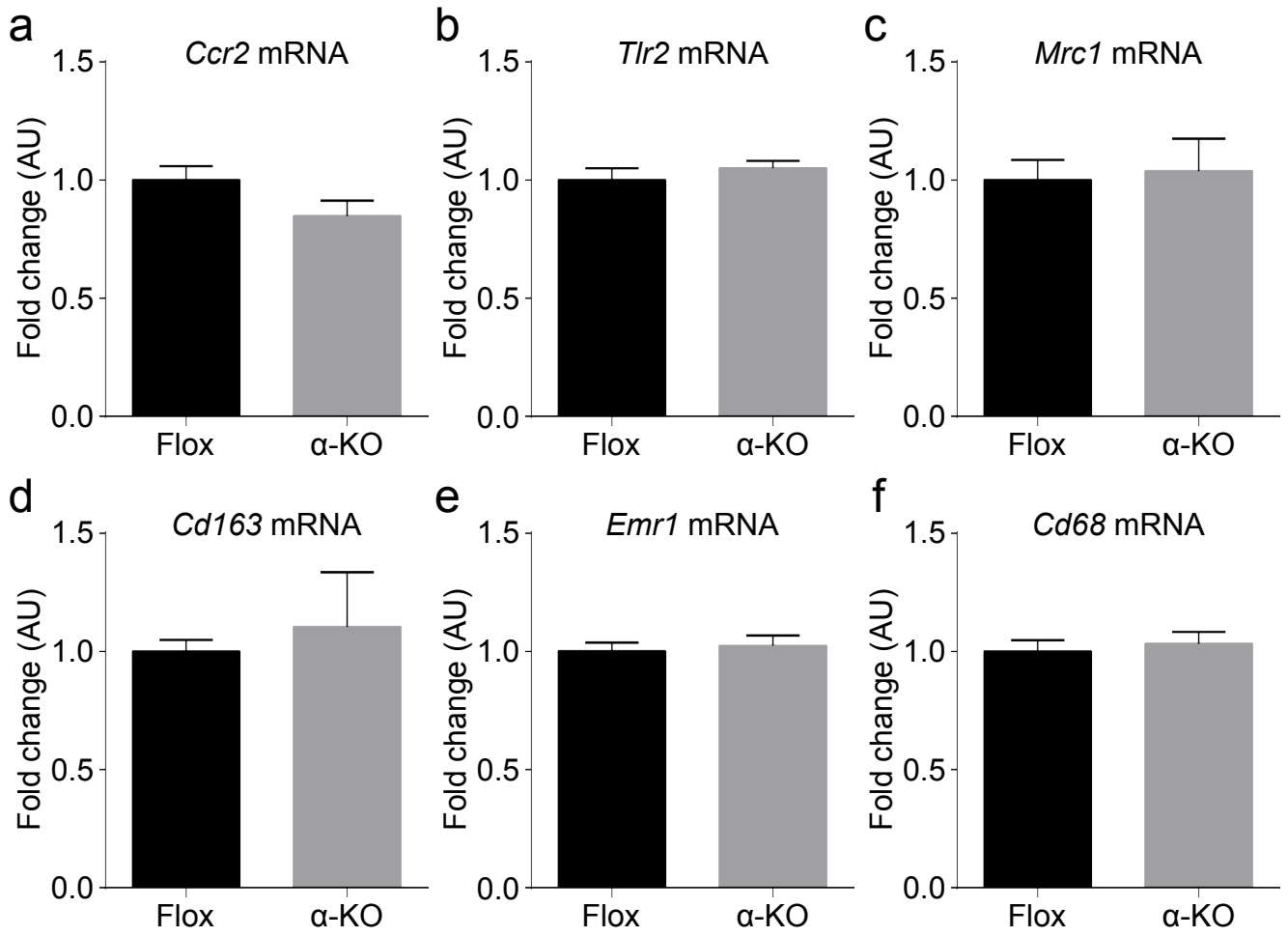
Supplementary Figure 2 | Characteristics of the systemic α -KO mice with sponge implantation. (a) Overview of the cut surface (upper) and H&E stained section (bottom) of the implanted sponge into Flox mice, excised after 14 days of implantation. The frame work of the sponge, corresponding to the translucent and angulated objects, was surrounded by connective tissues that grew into sponge. Connective tissue shows different types of cells, including fibroblasts, endothelial cells, and macrophages. Scale bars indicate 1 mm (a, upper) and 300 μ m (a, bottom). (b) Real-time PCR analyses of *Pdgfra* and *Pdgfrb* mRNA expression levels in Flox and α -KO mice of both sexes in implanted sponges; n = 4-5 per group. (c, d) Western blot analysis of PDGFR α (c) and PDGFR β (d) protein expression levels in Flox and α -KO mice of both sexes in implanted sponges; n = 4-5 per group. *, p < 0.05 versus Flox mice; **, p < 0.01 versus Flox mice; ***, p < 0.001 versus Flox mice; ****, p < 0.0001 versus Flox mice.



Supplementary Figure 3 | Angiogenesis is suppressed in implanted sponges in α -KO mice. (a, b) Immunohistochemical analysis of blood vessel formation in implanted sponge. Immunohistochemistry of collagen type IV (brown), a blood vessel specific extracellular matrix, in cross-sectional area of implanted sponges at day 14 after implantation. Boxed areas in (a) show as high magnification panels in (b) with the vascularized areas delineated by dotted lines. (c) Statistical analysis of the vascularized areas. Using Flox mice as the control (a, left), collagen type IV positive vascularized areas in α -KO (a, right) were examined in male at day 14 after implantation; n = 4 mice per group. *, p < 0.05 versus Flox mice. Scale bars indicate 1 mm (a) and 500 μ m (b), respectively.

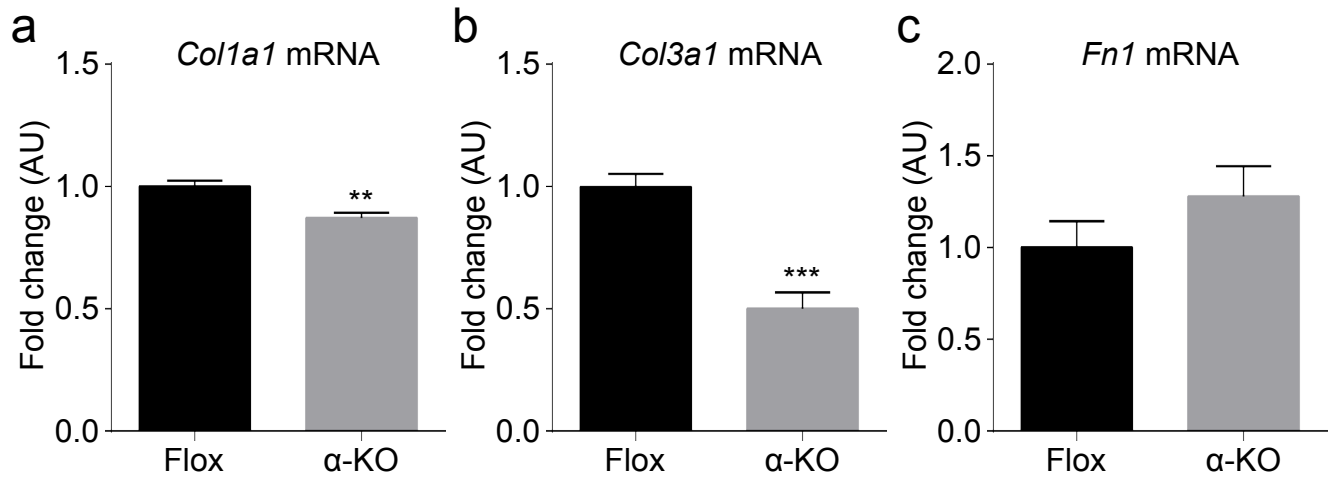


Supplementary Figure 4 | Cell division marker positive fibroblasts are decreased in implanted sponges in α -KO mice. (a) Immunofluorescence of phospho-histone H3 (pHH3), a M phase specific marker, in implanted sponges of Flox and α -KO mice. Number of dividing periostin-positive fibroblasts (yellow) that were co-labeled with pHH3 (green) were decreased in α -KO mice than in Flox mice (arrowheads). Infiltrating macrophages (red) were similar between the two genotypes. Nuclei are depicted by DAPI staining (blue). Scale bar indicates 20 μ m. (b, c) Morphometrical analysis of M phase (dividing) cells. The percentage of dividing fibroblasts (pHH3/periostin-positive) in periostin-positive fibroblasts is significantly less in α -KO mice than in Flox mice (b), but that of dividing macrophages (pHH3/MAC-2-positive) in MAC-2-positive macrophage is comparable between the two genotypes (c); n = 4 mice per group. ***, p < 0.001 versus Flox.

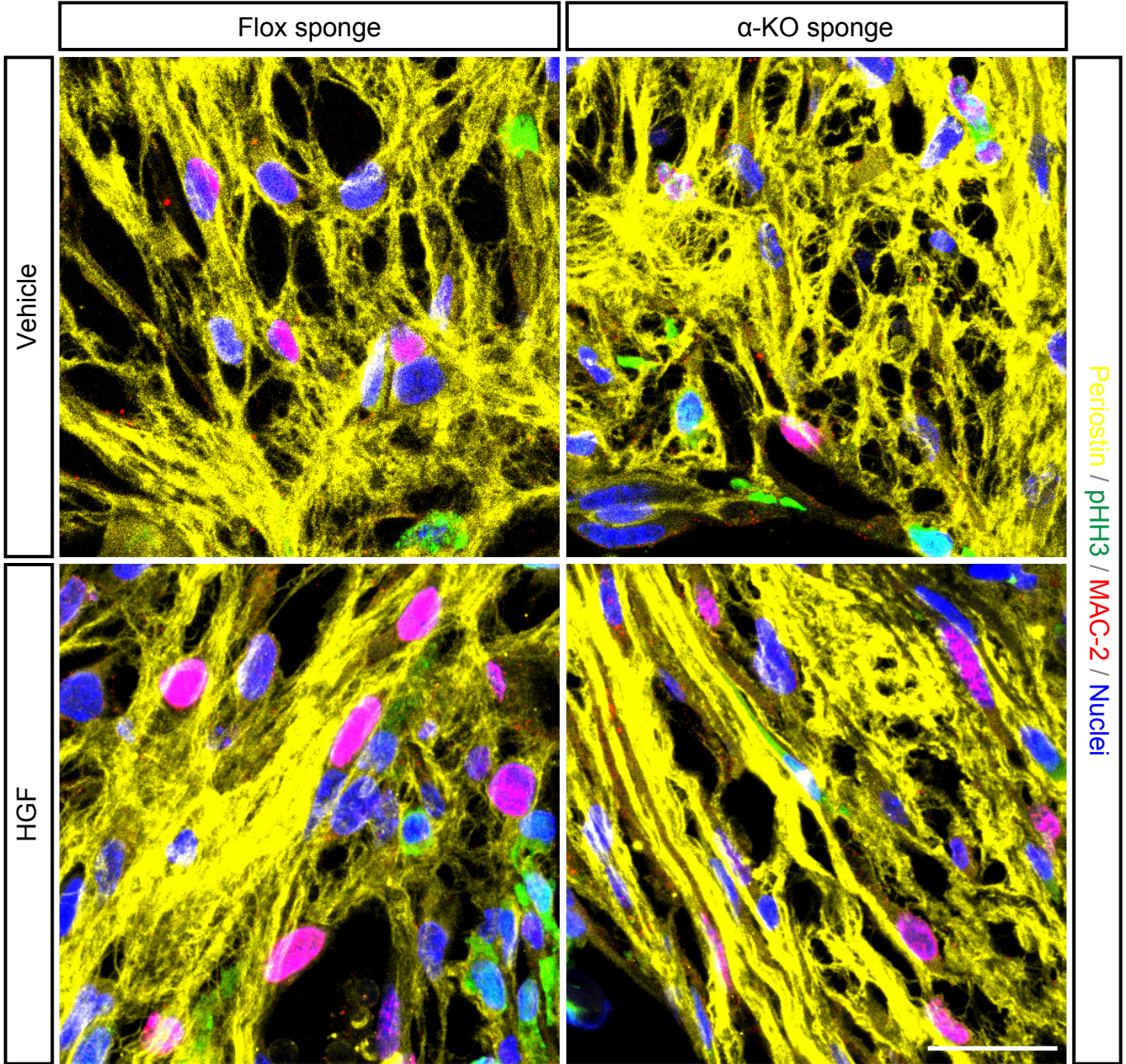


Supplementary Figure 5 | Infiltrating macrophages are comparable between two genotypes.

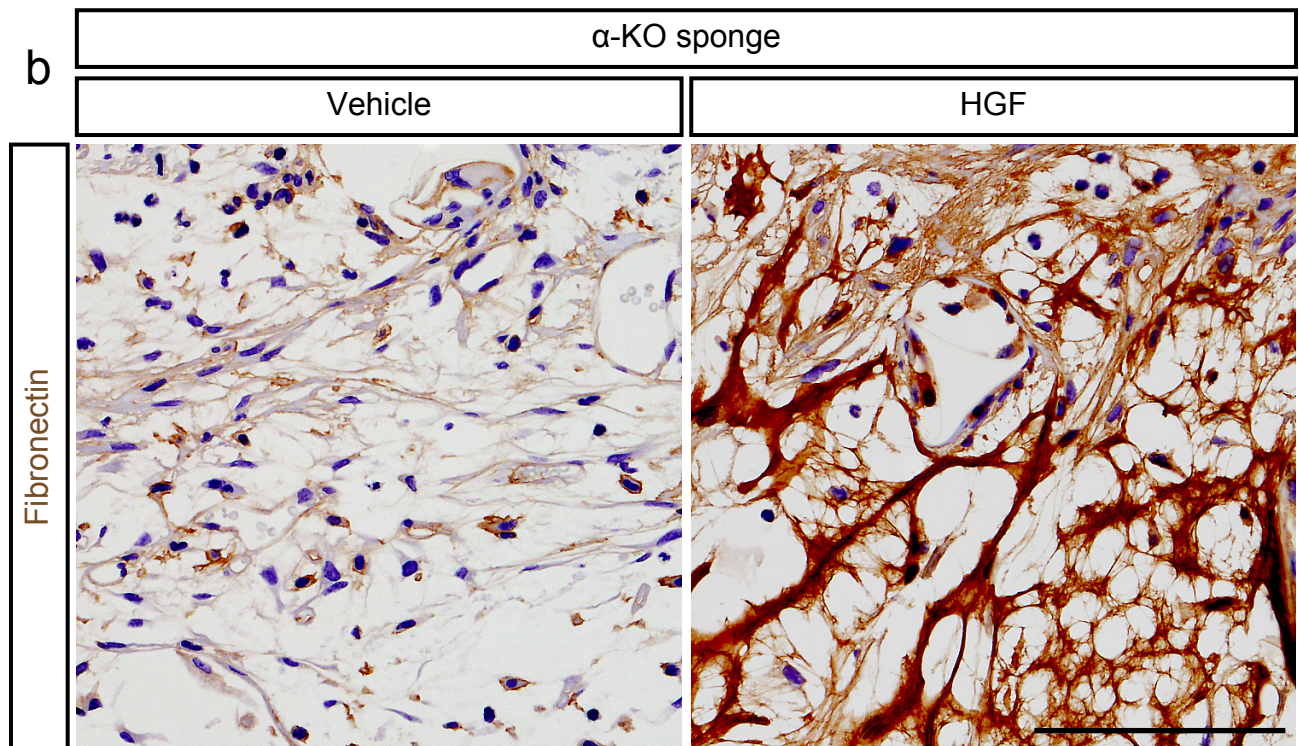
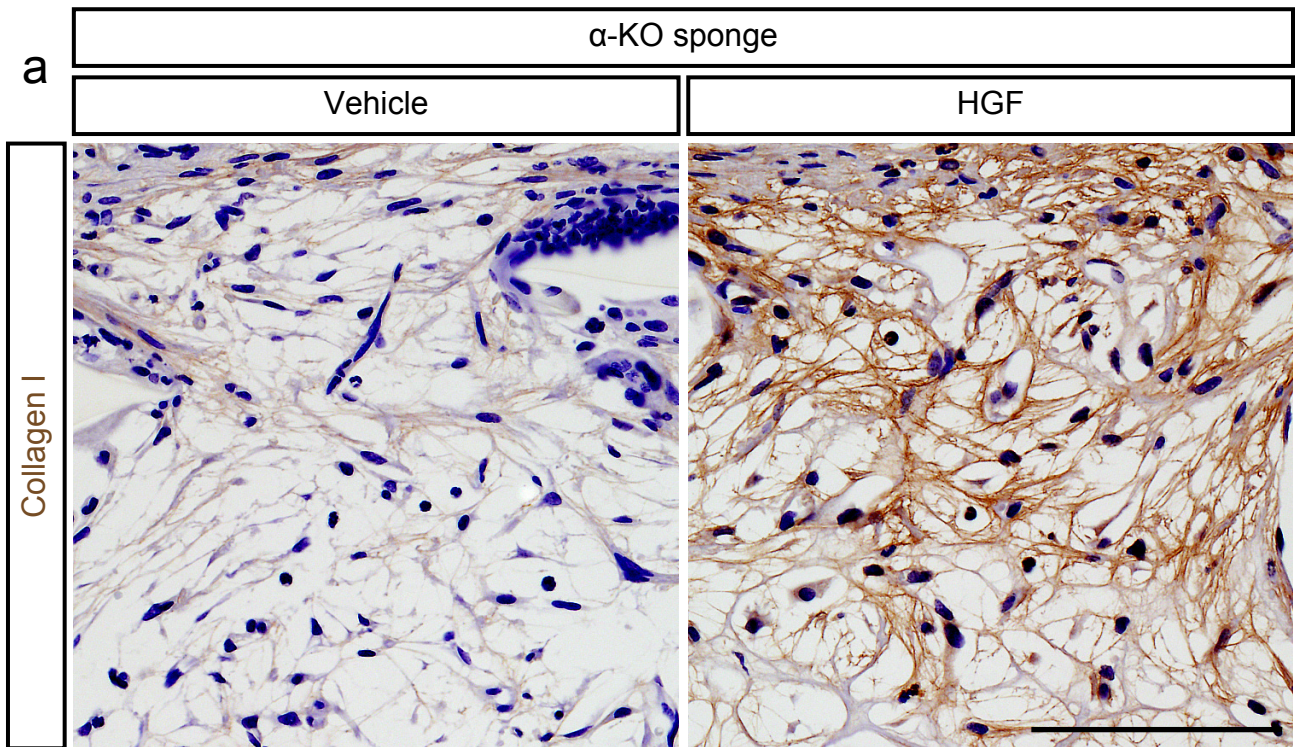
(a-f) Real-time PCR analyses of M1, M2 and pan-macrophage markers in implanted sponges; n = 4 per group. No significant difference can be observed in M1 (*Ccr2* and *Tlr2*; a, b), M2 (*Mrc1* and *Cd163*; c, d) and pan-macrophage markers (*Emr1* and *Cd68*; e, f). (g) VEGF-A (red), a potent angiogenic factor, expresses in MAC-2 positive infiltrated macrophages (green). Nuclei are depicted by DAPI staining (blue), and sponges are visible due to the autofluorescence (cyan). No significant difference in expression levels of VEGF-A can be seen between two genotypes. Scale bar indicates 50 μ m.



Supplementary Figure 6 | Collagen expression is significantly suppressed in α -KO fibroblasts.
(a-c) Real-time PCR analyses of *Coll1a1*, *Col3a1* and *Fn1* mRNA expression levels in Flox and α -KO fibroblasts; n = 6 per group. Expression levels of *Coll1a1* and *Col3a1* mRNAs are significantly suppressed in α -KO fibroblasts. In contrast, expression level of *Fn1* mRNA is comparable between two genotypes (n.s.). **, p < 0.01 versus Flox fibroblasts; ***, p < 0.001 versus Flox fibroblasts.



Supplementary Figure 7 | HGF promotes fibroblast proliferation in implanted sponges in α -KO mice. Immunofluorescence of ingrowing granulation tissue within the implanted sponges of Flox and α -KO mice, with or without HGF treatment. Periostin-positive fibroblasts (yellow) that are co-labeled with Ki67 (red) are increased in HGF treated groups. MAC-2 (green)-positive cells represent infiltrating macrophages into sponges. Increased proliferation of fibroblasts after HGF administration may suggest HGF plays a key role in fibroblast number in sponges. Nuclei are depicted by DAPI staining (blue). Scale bar indicates 20 μ m.



Supplementary Figure 8 | HGF promotes ECM deposition in implanted sponges in α -KO mice. (a) Immunohistochemistry of collagen type I in ingrowing granulation tissue within the sponges of α -KO mice with or without HGF treatment. HGF administration into sponges promotes collagen type I deposition. (b) Immunohistochemistry of fibronectin in ingrowing granulation tissue within the sponges of α -KO mice with or without HGF treatment. HGF administration into sponges promotes fibronectin deposition. Scale bar indicates 100 μ m.